ChemComm

COMMUNICATION

Dual catalysis mode for the dicarbonyl reduction catalyzed by diketoreductase†

Meiling Lu,‡[a] Yan Huang,‡[a] Mark A. White,‡[b] Xuri Wu,[a] Nan Liu,[a] Xiaodong Cheng*[bc] and Yijun Chen*[a]

Diketoreductase catalyzes a two-step bioreduction on a dicarbonyl substrate through a novel dual catalysis mode, in which random hydride attack simultaneously forms two mono-carbonyl intermediates, and subsequently distinct catalytic sites are responsible for the reductions of respective carbonyl group of the intermediates to yield the final dihydroxy product.

Dehydrogenase/reductase catalyzes stereoselective reduction of carbonyl groups in the presence of cofactor NAD(P)H. Thus far, most of the characterized dehydrogenases/reductases have been distributed into three superfamilies: aldo-keto reductase (AKR), short-chain dehydrogenase/reductase (SDR) and medium-chain dehydrogenase/reductase (MDR). Despite the similar enzymatic functions, the catalytic mechanisms of three superfamilies are distinct from each other. A common catalytic site of Tyr-Lys-Asp-His is identified in AKR superfamily;[1] the active site of SDR superfamily is formed by a triad/tetrad with highly conserved Tyr, Lys, Ser (and Asn), of which Tyr is the most conserved residue within the family;[2] and in MDR superfamily, the active site is composed of the triad of Gly-His-Glu or the tetrad of Asp-Glu-Asn-Thr depending upon the presence of Zn^{2+}.[3]

Different from typical dehydrogenase/reductase, there is another class of ketoreductase that can simultaneously reduce two carbonyl groups, namely dicarbonyl reductase.[4] The reduction of dicarbonyl compounds catalyzed by dicarbonyl reductases is a consecutive process with the formation of stable mono-carbonyl intermediates, and the final chiral diols are important in the regulation of metabolic function[5] and in the preparation of pharmaceutical intermediates.[4,6] To date, three dicarbonyl reductases, including sepiapterin reductase (SR),[7] α-acetoxy ketone reductase (Gre2p)[8]

and diketoreductase (DKR),[9] have been reported. SR and Gre2p belong to SDR superfamily, and their active sites are identified as Ser-Tyr-Lys.[10] The reduction of α,β-diketo substrates by SR could be explained by that it acts as both carbonyl reductase and isomerase.[11] Regarding the sequential reductions of 2,5-hexanedione by Gre2p[12] and ethyl 3,5-diketo-6-benzyloxy hexanoate (**1**) by DKR,[9] their catalytic mechanisms are unclear. In the case of DKR catalysis, the reduction of **1** involves the simultaneous formation of two iso-latable intermediates, (*S*)-ethyl6-(benzyloxy)-5-3-oxohexanoate (**2**) and (*R*)-ethyl6-(benzyloxy)-3-hydroxy-5-oxohexanoate (**3**), and further reduction to give chiral diol (3*R*, 5*S*)-ethyl6-(benzyloxy)-3,5-dihydroxy-hexanoate (**4**) (Scheme S1, ESI†),[13] which is useful for the preparation of statin drugs.[14] DKR is a homodimeric protein containing 283 amino acid residues, and it shares an amino acid sequence identity of 35.7% with human heart 3-hydroxyacyl-CoA dehydrogenase (HAD), an enzyme important to oxidative fatty-acid metabolism in mammals.[15] Based on the crystal structure of the HAD/NAD$^+$/acetoacetyl-CoA ternary complex, the catalytic mechanism of HAD was proposed.[16] However, HAD was unable to reduce the dicarbonyl substrate **1**, and DKR could not act on the HAD substrate acetoacetyl-CoA. Although the previous mutagenesis study based on modeled structure has identified that His143, Ser122 and Glu155 play critical roles in DKR catalysis,[17] a number of important issues regarding the complex catalytic process, such as why is a two-step reduction, whether the two steps are identical, how to simultaneously reduce two carbonyl groups and whether the same catalytic site works on different carbonyl groups, remain elusive. In the present study, we combined structural determination, molecular docking and biochemical analyses to elucidate the two-step dicarbonyl reduction process of DKR.

Crystal structures of apo-DKR, the NADH, and NAD$^+$ binary complexes were solved at resolutions of 1.9–2.1 Å using the heavy-atom salt derivative method (PDB codes 4E12, 4E13, and 4DYD).[18] Data of crystallographic analysis are summarized in Table S1 (ESI†). DKR exists as a symmetric homodimer in all the crystal structures (Fig. S1, ESI†), indicating that the two subunits possess exactly the same structure and they should function identically.

The DKR subunit consists of two distinct domains: N-terminal domain α/β dinucleotide-binding domain (residues 1–183) and C-terminal α-helical domain (residues 192–283). The N-terminal

[a] Laboratory of Chemical Biology and State Key Laboratory of Natural Medicines, China Pharmaceutical University, 24 Tongjia Street, Nanjing, Jiangsu Province 210009, People's Republic of China. E-mail: yjchen@cpu.edu.cn; Fax: +86 25 83271031; Tel: +86 25 83271045
[b] Sealy Center for Structural Biology and Molecular Biophysics, The University of Texas Medical Branch, Galveston, Texas 77555–0857, USA
[c] Department of Pharmacology and Toxicology, The University of Texas Medical Branch, Galveston, Texas 77555–0857, USA. E-mail: xcheng@utmb.edu
† Electronic supplementary information (ESI) available: The details of methods and supplementary figures and tables. See DOI: 10.1039/c2cc36334h
‡ These authors contributed equally to the work.

domain contains eight β-strands (β1–β8) and seven α-helices (α1–α7), and displays a typical Rossmann fold containing an α/β dinucleotide binding motif, which is the common structural feature of SDR superfamily. The C-terminal domain of DKR adopts an entirely helical architecture responsible for the subunit dimerization, and presumably binds substrate **1**. The two domains are connected by a short linker region (residues 184–191), which appears to be important in correctly positioning active site residues (Fig. S1, ESI†). Structural search using the DALI server[19] revealed considerable similarity between the N-terminal domain of DKR and a number of oxidoreductases: human HAD (PDB code 1F0Y; Z-score = 32.9; rmsd = 2.5 Å), rabbit L-gulonate 3-dehydrogenase (PDB code 3ADO; Z-score = 27.6; rmsd = 2.5 Å) and *Aquifex aeolicus* prephenate dehydrogenase (PDB code 2G5C; Z-score = 18.2; rmsd = 4.2 Å).

Among these structures, the global fold and dimerization of DKR exhibit the closest overall similarity with human HAD.[15,16] However, the presence of a unique Trp149 in DKR may result in no catalytic activity of DKR towards acetoacetyl-CoA by preventing the binding with the active site (Fig. S2, ESI†). Additionally, the major structural differences between the two enzymes, such as cofactor binding-induced conformational change (Fig. S3, ESI†) may contribute to their respective binding and catalysis.

A putative active site was identified to be an inter-domain pocket that is adjacent to the nucleotide-binding site (Fig. S1, ESI†), in which the nicotinamide moiety of NADH and catalytically important residues Ser122, His143 and Glu155 are found. Even though these structural features were consistent with previous results of site-directed mutagenesis based on the modeled structure,[17] a single active site in the DKR molecule was unable to reasonably explain the two-step process and the reduction of both β- and δ-carbonyl groups.

In order to identify more residues possibly involved in the catalytic process, molecular docking and molecular dynamics simulation were employed to probe the interaction between DKR and the substrate **1**. The orientation of substrate **1** was found to be stabilized by two groups of hydrogen bonding: one between the β-carbonyl group and the side chains of Ser122, His143, Glu155 and Asn194; and the other between the δ-carbonyl group and the side chains of Asn146, His147 and Asn151 (Fig. S4, ESI†). According to the interaction, there could be two separate catalytic sites as represented by the

two hydrogen bonding clusters in each subunit. Then, it is conceivable that inactivation of one catalytic site by mutagenesis would produce variants with a preference for the reduction of a specific carbonyl group in substrate **1**. Surprisingly, mutations of Ser122, His143 or Glu155 led to a complete inactivation of the enzyme, and neither intermediate was produced. In addition, mutants H147A/K and N151A/Q remained active towards both β- and δ-carbonyl groups (Table S2, ESI†). These results suggested that Ser122, His143, and Glu155 are clustered to form a catalytic center responsible for the reduction of both β- and δ- carbonyl groups of substrate **1**.

Given that the intermediates **2** and **3** simultaneously appeared in the first step,[13] the transfer of protons/hydrides to substrate **1** has to be a random process, which is supported by the keto–enol tautomerization of substrate **1** clearly observed from ^{1}H NMR (Fig. S5 and S6, ESI†).[13] Under the optimal DKR catalytic condition (pH 6.0), keto–enol is the dominant form with a 6-membered ring formed through intra-molecular hydrogen bonds. Therefore, we used structure **5** instead of **1** to dock with the binary complex structure of DKR to investigate how two intermediates are generated synchronously in the first reduction step.

As shown in Fig. 1a and S7 (ESI†), compound **5** fits into the active site cleft and its 6-membered keto–enol ring lies between the imidazole ring of His143 and the B-side of the nicotinamide of NADH. Hydrogen bonds are formed between Ser122 and α-carboxylic oxygen, between Ser122/His143/Asn194 and the β-carbonyl oxygen, and between Asn146 and the δ-hydroxyl group. Additional hydrogen bonds are also found in the pairs of His143/Glu155, His147/Asn151, as well as Asn146/His147. These hydrogen bonds are crucial for the catalysis because variants such as S122K/T, H143N/Q and E155D/S completely lost their catalytic activities towards both mono-carbonyl intermediates **2** and **3** (Table S2, ESI†). Since the protonation of His143 is absolutely required for the formation of a reactive E-NADH-substrate **1** complex, a catalytic triad consisting of Glu155, His143 and Ser122 is very likely to be connected by a hydrogen bonding network for the catalytic cycle (Fig. 1b). After the protonation of His143 with the assistance of Ser122 and Glu155, partially negative charged oxygen of the β-carbonyl group of **5** occurs during the transition state stabilized by the positive charge of the protonated imidazole ring. Meanwhile, the intra-molecular electron transfer of the enol substrate
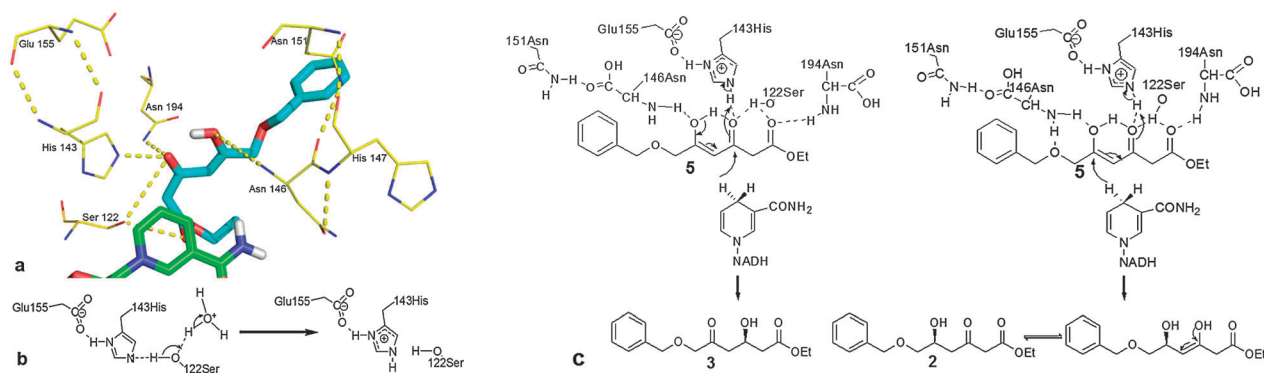

Fig. 1 The first step reduction of substrate **1**. (a) Hydrogen-bonding network of substrate **1** as keto–enol form **5** in the DKR active site. The keto–enol form (**5**) of substrate **1** and the partial NADH molecule are colored in cyan and green, respectively. Hydrogen bonds are shown as yellow dashed lines. (b) Drawing of the protonation of His143 in the DKR active site. (c) Proposed mechanism for the first step reduction of substrate **1**.
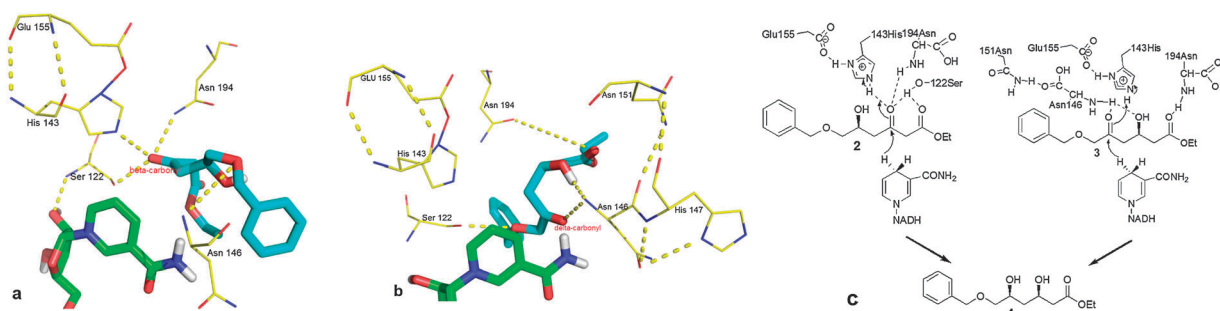
Fig. 2 The second step reduction of substrate **1**. (a) Hydrogen-bonding network of the intermediate **2** in the DKR active site. Intermediate **2** and the partial NADH molecule are colored in cyan and green, respectively. Hydrogen bonds are shown as yellow dashed lines. (b) Hydrogen-bonding network of the intermediate **3** in the DKR active site. Intermediate **3** and the partial NADH molecule are colored in cyan and green, respectively. Hydrogen bonds are shown as yellow dashed lines. (c) Proposed mechanism for the second step reduction of substrate **1**.

with a conjugated aromatic system leads to electron-deficiency at either the β- or the δ-position, both of which are prone to nucleophilic attack by the hydride from NADH, with a similar distance of 3.2 Å or 3.8 Å to the β- or δ-carbonyl, respectively. Consequently, a random transfer of a hydride allowed the generation of two different mono-carbonyl intermediates in the first step of reduction by DKR (Fig. 1c).

Because residues Asn146, His147, Asn151 and Asn194 are potentially involved in the catalysis based on the docking results, mutations of these residues were performed. After mutagenesis, H147A/K, N151A/Q and N194A exhibited notable activity towards substrates **1**, **2**, and **3**. In contrast, variants of Asn146 showed a pronounced substrate preference, nearly inactive to **3** while retaining comparable activity to **2** as shown in Table S2 (ESI†). This indicated that Asn146 indeed participates in the reduction of the δ-carbonyl group in the second step. Docking models showed that the β-carbonyl group of **2** is close to the nicotinamide ring of NADH, in which the β-carbonyl oxygen faces His143. However, the distorted orientation of the δ-hydroxyl group disrupted the hydrogen bonding between the hydroxyl group and Asn146 but facilitated the hydrogen bonding between Asn146 and the oxygen linked to the benzoyl moiety (Fig. 2a and S8 (ESI†)), which is consistent with the mutagenesis data of Asn146. During the reduction of intermediate **2**, the catalytic triad consisting of Glu155, His143, and Ser122 was the same as the one in the first step, in which the hydrogen bond between the hydroxyl group of Ser122 and β-carbonyl stabilizes the transition state, and the polarized β-carbonyl group is then reduced after accepting a proton from His143. On the other hand, mono-carbonyl intermediate **3** showed an inverted binding orientation, in which the carbonyl oxygen at the δ-position is closer to His143 and Asn146 (Fig. 2b and S9, ESI†). The striking preference of Asn146 for **3** suggested that Asn146 interacts with the δ-carbonyl group of intermediate **3**. Because of the far/close distance from Ser122/Asn146 to the δ-carbonyl group, Asn146 played a similar role as Ser122 in the β-carbonyl reduction to form a hydrogen bond for the stabilization of the transition state. The interaction between Asn146 and the δ-carbonyl group promoted the polarization of the carbonyl moiety for the transfer of protons and hydrides. As a result, a catalytic tetrad consisting of Ser122-Asn146-His143-Glu155 was responsible for the δ-carbonyl reduction of **3** (Fig. 2c).

The present study unveiled that DKR catalyzes a stepwise double reduction by random hydride attack from NADH in the first-step of the reduction, and the involvement of two distinct catalytic clusters in the subsequent reductions of the mono-carbonyl intermediates. The present dual catalysis mode is the first example in enzyme catalysis, which provides new insights into how an enzyme catalyzes complex reactions and will facilitate the rational design of novel enzymes for various functions.

Notes and references

1 (a) R. Kratzer, D. K. Wilson and B. Nidetzky, *IUBMB Life*, 2006, **58**, 499; (b) M. Klimacek, M. Szekely, R. Griessler and B. Nidetzky, *FEBS Lett.*, 2001, **500**, 149; (c) S. Leitgeb, B. Petschacher, D. K. Wilson and B. Nidetzky, *FEBS Lett.*, 2005, **579**, 763.
2 (a) A. M. Lesk, *Curr. Opin. Struct. Biol.*, 1995, **5**, 775; (b) N. Tanaka, T. Nonaka, K. T. Nakamura and A. Hara, *Curr. Org. Chem.*, 2001, **5**, 89.
3 E. Nordling, H. Jornvall and B. Persson, *Eur. J. Biochem.*, 2002, **269**, 4267.
4 Y. Chen, C. Chen and X. Wu, *Chem. Soc. Rev.*, 2012, **41**, 1742.
5 S. Supangat, *et al.*, *J. Biol. Chem.*, 2006, **281**, 2249.
6 Y. Huang, N. Liu, X. Wu and Y. Chen, *Curr. Org. Chem.*, 2010, **14**, 1447.
7 B. Thöny, G. Auerbach and N. Blau, *Biochem. J.*, 2000, **347**, 1.
8 M. Müller, M. Katzberg, M. Bertau and W. Hummel, *Org. Biomol. Chem.*, 2010, **8**, 1540.
9 (a) X. Wu, N. Liu, Y. He, Y. Chen, 2008, http://hdl.handle.net/10101/npre.2008.1697.1; (b) X. Wu, N. Liu, Y. He and Y. Chen, *Acta Biochim. Biophys. Sin.*, 2009, **41**, 163.
10 (a) K. M. Fujimoto, *et al.*, *Chem.–Biol. Interact.*, 2001, **130–132**, 825; (b) B. Persson, *et al.*, *Chem.–Biol. Interact.*, 2009, **178**, 94.
11 (a) G. Auerbach, *et al.*, *EMBO J.*, 1997, **16**, 7219; (b) S. Katoh and T. Sueoka, *J. Biochem.*, 1987, **101**, 275.
12 K. Breicha, M. Müller, W. Hummel and K. Niefind, *Acta Crystallogr., Sect. F: Struct. Biol. Cryst. Commun.*, 2010, **66**, 838.
13 (a) Z. Guo, Y. Chen, A. Goswami, R. L. Hanson and R. N. Patel, *Tetrahedron: Asymmetry*, 2006, **17**, 1589; (b) X. Wu, C. Chen, N. Liu and Y. Chen, *J. China Pharm. Univ.*, 2010, **41**, 408.
14 (a) X. Wu, L. Wang, S. Wang and Y. Chen, *Amino Acids*, 2010, **39**, 305; (b) X. Wu, C. Chen, N. Liu and Y. Chen, *Bioresour. Technol.*, 2011, **102**, 3649; (c) X. Wu, J. Jiang and Y. Chen, *ACS Catal.*, 2011, **1**, 1661.
15 J. J. Barycki, *et al.*, *Biochemistry*, 1999, **38**, 5786.
16 J. J. Barycki, L. K. O'Brien, A. W. Strauss and L. J. Banaszak, *J. Biol. Chem.*, 2000, **275**, 27186.
17 Y. Huang, Z. Lu, N. Liu and Y. Chen, *Biochimie*, 2012, **94**, 471.
18 M. A. White, *et al.*, *Acta Crystallogr., Sect. D: Biol. Crystallogr.*, 2008, **64**, 487.
19 L. Holm and C. Sander, *J. Mol. Biol.*, 1993, **233**, 123.